Dynamic Characteristics of a New Electrical Toothed Band Brake

LI Chao[1], *LI Kai*[1], *CHEN Man*[1*], *FAN Ye*[1], *ZHOU Ruyi*[2], *LU Weichen*[3]

1. School of Mechanical Engineering, Beijing Institute of Technology, Beijing 100081, P. R. China;
2. China North Vehicle Research Institute, Beijing 100072, P. R. China;
3. Shanghai Marine Diesel Engine Research Institute, Shanghai 201108, P. R. China

(Received 2 November 2024; revised 17 March 2025; accepted 22 March 2025)

Abstract: A new electrical toothed band brake is proposed based on the planetary gear shifting transmission. The corresponding mathematical model and the finite element model are established to investigate the braking dynamic characteristics and the stress distribution of brake components. According to the structural features and working principle of the brake, the braking process can be divided into a gap elimination stage, a sliding stage, a meshing stage, and a collision stage. The greater the initial speed of brake drum, the higher the impact torque in the collision stage, and the larger the stress of brake components. The ideal range of initial speed is 50—100 r/min, and the ultimate stress is 514 MPa appeared in the right brake band. This study present a wide range of possibilities for further investigation and application of the electrical toothed band brake.

Key words: toothed band brake; electrically control; braking characteristics; rotating speed; impact torque

CLC number: U463.2 **Document code:** A **Article ID:** 1005-1120(2025)05-0629-09

0 Introduction

The wet multi-disc brake is commonly used in the planetary gear shift transmission system of the heavy load vehicles. It relies on the friction between fixed end and active end to brake[1-2]. In order to ensure the braking reliability, a large pressure should be applied between the friction pairs, which is usually completed by the hydraulic actuator[3]. Therefore, such a brake needs to be equipped with a large volume and weight of the hydraulic system. Plus, the friction components in the brake are prone to the thermal buckling or wear failure in some severe working conditions, resulting in unstable working performance and even loss of braking ability[4-5]. There is an urgent need to improve the transmission mechanism of the planetary gear shifting transmission system, so that it can adapt to complex and harsh working conditions

Scholars worldwide have conducted considerable studies on the braking device of planetary gear transmission[6]. To optimize braking performance, Hu et al.[7] conducted in-depth research on the influence of braking parameters such as gear braking force, relative speed difference, and relative rotation angle on the shifting quality of stepped transmissions. On this basis, Shin et al.[8] designed a two-speed shifting gear mechanism using the Simpson type planetary gear system, and experimentally verified key aspects such as gear strength, meshing efficiency, and transmission efficiency, improving the practicality of gear mechanism design. In the field of dynamic modeling and clutch engagement, Rahimi Mousavi et al.[9] developed a dynamic model for electric vehicles based on torque balance and virtual work principle, combined with two-stage planetary gear sets and two braking devices, effectively controlling power flow. Bóka et al.[10] then focused on the meshing uncertainty in the toothed clutch of heavy-duty vehicle automatic transmission (AMT), using a mechanical model to describe this uncertainty as a function of initial speed difference and deter-

*Corresponding author, E-mail address: turb911@bit.edu.cn.

How to cite this article: LI Chao, LI Kai, CHEN Man, et al. Dynamic characteristics of a new electrical toothed band brake [J]. Transactions of Nanjing University of Aeronautics and Astronautics, 2025,42(5):629-637.

http://dx.doi.org/10.16356/j.1005-1120.2025.05.006

mining the probability of successful meshing. Duan[11] simulated the shifting process of a six-speed automatic transmission by constructing a physical model of a toothed clutch, and confirmed the feasibility of the model through comparison with dynamometer data. Regarding brake performance improvement and new brake design, Andersson et al.[12] modified the shape of the teeth of the embedded clutch in all-wheel drive vehicles, leading to a substantial increase in the maximum allowable engaging speed difference from 50 r/min to 120 r/min as demonstrated by the finite element simulation. Han et al.[13] investigated the impact of different brake lining shapes and distributions on marine winch brake performance, while Downey et al.[14] applied high-performance controllable damping devices to structural systems for disaster mitigations and proposed a novel semi-active damping device based on the belt brake to reduce costs. Li et al.[15] developed a toothed band brake that occupied less space and was lighter in weight compared to multi-disc brakes, as well as eliminated oil drag torque, leading to a significant step forward in brake design. Ma et al.[16] continued this line of research by further improving the toothed band brake to achieve a wider speed range, which was successfully verified by bench tests. In summary, current research lacks theoretical research on toothed belt brakes.

This paper proposes a mathematical model and a finite element model of the toothed band brake to study the braking characteristics and stress distribution. Through this study, the working characteristics, component stress characteristics and influencing factors of the brake during braking can be obtained. Further, this study provides a theoretical basis for the subsequent structural improvement of the brake, and technical referrence for the research and development of all electric transmission mechanism.

1 Methodology

1.1 Structural features and working principle

The toothed band brake is shown in Fig.1. Its feasibility and applicability have been verified in our previous research via the bench experiments[16]. Since the toothed band brake is symmetrical, and the braking process is analyzed only by the left brake belt. The motors on the left and the right sides are used to drive the fork shaft, thereby driving the brake belt movement. During the braking process, the actuator motor drives brake band to move along the fork shaft. The brake impact torque is transferred by the collision between the brake band and the brake drum. Moreover, each brake band has two active ends, thus allowing for shorter movement distances and braking duration. The brake drum is actually the ring of the planetary gear train. Since the brake band is made of rigid material, its movement can be equivalent to a horizontal movement near or away from the center of the brake drum. Four teeth are evenly distributed along the circumferential direction of the brake band and brake drum. The inner teeth of brake band are connected with the outer teeth by bolts. The friction force between the brake band and the teeth can be changed by adjusting the pre-tightening force of bolts to absorb the kinetic energy of the brake drum. The moving end of the brake band teeth is fitted with a limit bolt, which prevents the spring from moving in the non-axial direction, and withstands the collision of the brake teeth. The brake belt teeth are connected with two springs, as when the brake drum teeth collide with the brake belt teeth, the two springs produce a tension and a pressure, which increases the motion resistance of the brake drum teeth. The two springs also facilitate the rapid return of the brake band teeth.

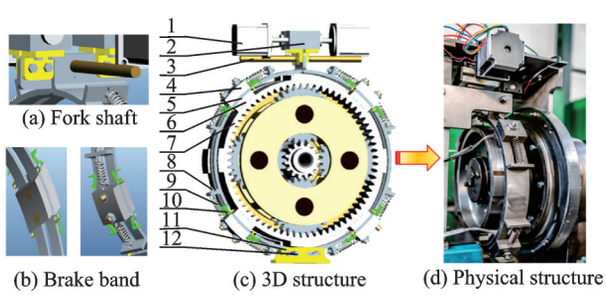

1—Actuator motor, 2—Screw-nut, 3—Fork shaft, 4—Outer tooth, 5—Brake band, 6—Inner tooth, 7—Brake drum, 8—Limit bolt, 9—Spring, 10—Self-locking steel sheet, 11—Supporter, 12—Slider pin

Fig.1 Structure of toothed band brake

The working process of the toothed band brake is shown in Fig.2. Since the four teeth on the brake band have similar working conditions, only one of them is analyzed in dynamics. As shown in Fig.2 (a), when brake starts, the brake band approaches the brake drum horizontally, and the gap elimination stage starts. More exactly, the gap between the brake band and the brake drum is gradually eliminated until the teeth contact the brake drum. As illustrated in Fig.2(b), the sliding stage can be divided into the tooth top sliding stage or the tooth bottom sliding stage. If the brake band teeth are in touch with the brake drum teeth, the tooth top sliding stage is coming; otherwise, the tooth bottom sliding happens. As for the meshing stage shown in Fig.2(c), the brake drum drives the brake band teeth to move together, while its rotating speed decays dramatically under the action of the spring and friction resistance. When the spring is compressed to the limit, the collision phase comes. The instantaneous collision between the brake drum and the brake band directly causes its speed to drop to 0, thus completing the braking process.

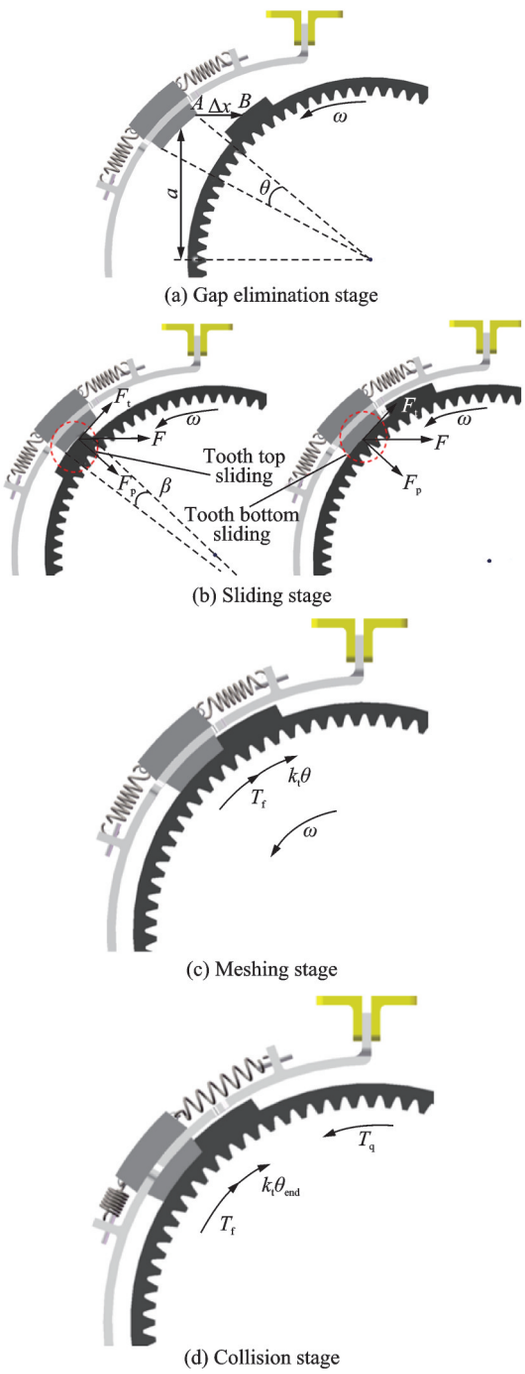

Fig.2 Working principle of toothed band brake

1.2 Mathematical model

1.2.1 Gap eliminating stage

As shown in Fig.3(a), since the displacement of the brake teeth Δx are the same as that of the screw nut, the moving velocity can be expressed as

$$v = \frac{Dn}{60} \tag{1}$$

where n is the rotating speed of motor and D the lead of screw.

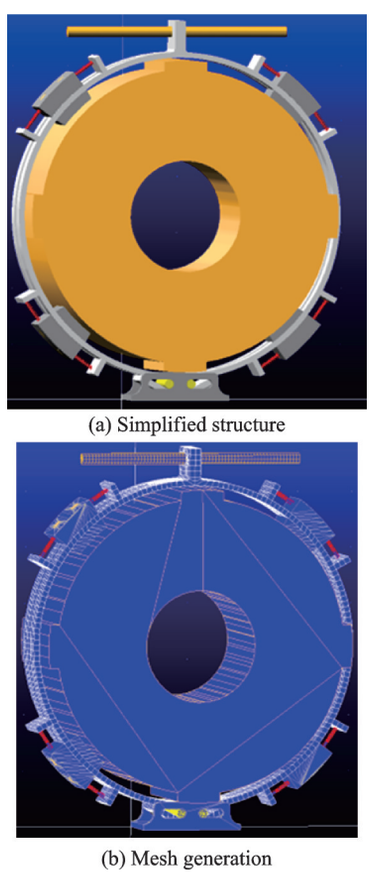

Fig.3 Finite element model of brake

Assuming that the brake drum undergoes the resistance load T_N, its angular acceleration can be given as

$$\alpha_0 = \frac{T_N}{J_r} \tag{2}$$

where J_r is the inertia of transmission system.

Integrating Eqs.(1—2), the angular velocity of the brake drum at the end of the gap eliminating stage can be obtained as

$$\omega_1 = \omega_0 - \frac{60\alpha_0 \Delta x}{Dn} \tag{3}$$

1.2.2 Sliding stage

The maximum sliding angle of the tooth A on the top(bottom) of tooth B is given as[17]

$$\theta_{top} = \theta + 2\arctan\left(\frac{r\sin\frac{\theta}{2}}{r + \Delta x\cos\left(\frac{\pi}{4} + \frac{\theta}{2}\right)}\right) + 2\arctan\left(\frac{\Delta x}{\Delta x + 2a}\right) \tag{4}$$

$$\theta_{bot} = \frac{\pi}{2} - 2\theta - \int \omega \mathrm{d}t \tag{5}$$

where θ is the central angle of the tooth A and tooth B; r the inner radius of the bake drum; and a the vertical distance from the band tooth to the center of the brake drum.

The brake band will exert a large friction force on the brake drum to hinder its rotating

$$f = 2\mu F\cos\left(\frac{\pi}{4} - \beta\right) \tag{6}$$

where μ is the coefficient of friction(COF); β the central angle of the tooth contact area; and F the motor thrust.

Thus, the resistance torque of brake drum can be expressed as

$$T_f = f(r + h) \tag{7}$$

Thus, the angular velocity of brake drum can be obtained as

$$\omega_2 = \omega_1 - \int_0^{t_2} \frac{(T_N + T_f)}{J_r} \mathrm{d}t \tag{8}$$

1.2.3 Meshing stage

The motion of the brake drum and band teeth during the meshing stage can be considered as the torsional vibration of a single degree of freedom system under the impact load, which can be expressed as

$$J\theta'' + k_t\theta + T_f = 0 \tag{9}$$

where J and T_f are the rotational inertia and friction torque of the brake, respectively; k_t is the torsional stiffness.

The teeth are in a static state before the meshing stage, and then start moving under the momentum moment applied by the brake drum, where the initial condition is

$$\begin{cases} \theta(t=0) = \theta_0 = 0 \\ \theta'(t=0) = \theta_0' = \dfrac{J_q\omega_2}{J} \end{cases} \tag{10}$$

where J_q is the rotational inertia of the brake drum.

If the initial speed of brake drum is small, it will stop rotating before the spring reaches the maximum compression; otherwise, the spring will be completely compressed, resulting in a collision between the brake band and the brake drum. For the former, when the brake band stops rotating, the rotation angle reaches the peak and can be obtained as

$$\theta_{max} = \frac{1}{k_t}\left(\sqrt{T_f + J_q k_t \omega_2^2} - T_f\right) \tag{11}$$

$$|\theta''_{max}| = \frac{1}{J_q}\sqrt{T_f^2 + J_q k_t \omega_2^2} \tag{12}$$

When the brake drum stops rotating, the shift process is completed and the motor will restore the torque T_q. Meanwhile, the brake drum will continue to move until the spring is completely compressed, and the final rotation angle of the brake drum is obtained as

$$\begin{cases} \theta(t_{end}) = A_1\cos\omega_n t + \dfrac{T_q'}{k_t} = \theta_{end} \\ \theta'(t_{end}) = -A_1\omega_n\sqrt{1 - \dfrac{\left(\theta_{end} - \dfrac{T_q'}{k_t}\right)^2}{A_1^2}} \\ \theta''(t_{end}) = \dfrac{T_q' - k_t\theta_{end}}{J} \end{cases} \tag{13}$$

where $T_q' = T_q - T_f$, $\omega_n = \dfrac{k_t}{J}$, $A_1 = \theta_{max} - \dfrac{T_q'}{k_t}$.

For the latter, the brake drum will rotate to the maximum compression of spring, and the angular velocity is

$$\begin{cases} \theta'(t_{\text{end}}) = \rho\omega_n \sqrt{1 - \left(\dfrac{\theta_{\text{end}} k_t + T_f}{k_t \rho}\right)^2} \\ \theta''(t_{\text{end}}) = -\dfrac{1}{J}(k_t \theta_{\text{end}} + T_f) \end{cases} \tag{14}$$

where $\rho = \sqrt{A_1^2 + A_2^2}$, $\alpha = \arctan\left(\dfrac{A_1}{A_2}\right)$, $A_2 = \dfrac{\omega_2}{\omega_n}$.

The angular velocity of brake drum at the end of the meshing stage can be given by

$$\omega_3 = \theta'(t_{\text{end}}) \tag{15}$$

1.2.4 Collision stage

The impact torque T_I of brake drum can be written as

$$\int T_I \mathrm{d}t = \int (T_q - T_f - k_t \theta_{\text{end}}) \mathrm{d}t + J\omega_3 \tag{16}$$

Since the collision process is as short as 10^{-1}—10^{-4} s, Eq.(16) can be simplified as

$$T_I = T_q - T_f - k_t \theta_{\text{end}} + \frac{J\omega_3}{\Delta t} \tag{17}$$

In order to ensure the minimum impact torque, the brake drum should make the spring fully compressed with a brake torque of 0. Thus, the minimum speed of the brake drum in the early meshing stage can be expressed as

$$\omega_{2\min} = \sqrt{\frac{(k_t \theta_{\text{end}} + T_f)^2 - T_f}{J_q k_t}} \tag{18}$$

1.3 Finite element model

As shown in Fig.3, a simplified finite element model of the toothed band brake is developed to study the braking performance and stress distribution, which involves the following steps. First, the 3D assembly model is established. The planetary row is simplified as a rigid disk, and its size and rotational inertia remains unchanged at 0.4 kg•m^2. Second, the 3D assembly model is imported into Adams, and the material properties, constraints, contact, load and other physical elements are defined. Then a multi-rigid body dynamic model is generated as show in Fig.3(a). Third, the left and the right brake belts as well as the fork shaft and pins are flexible. More exactly, all components are meshed in hexahedral uncoordinated mode unit (C3D8I) with the integral solver Hilbert-Hughes-Taylor (HHT). The numbers of the unit and the node of each component are listed in Table 1. The simulation step is 4e−5. Since the brake failure mainly occurs in the collision stage, the stress characteristics of the vulnerable components are analyzed, including the brake bands, fork shaft and slider pins.

Table 1 Meshing method of components

Component	Unit size/mm	Unit	Node
Brake band	5	885	2 145
Fork shaft	3	670	1 088
Slider pin	2	525	728

2 Results and Discussion

The ideal braking process should involve the tooth tip sliding stage and the tooth bottom sliding stage. All-tooth meshing should be maintained during the meshing stage. The brake parameters selected are shown in Table 2. The initial speed of the brake drum is set to 30, 75 and 120 r/min.

Table 2 Braking parameters

Parameter	Value
Brake drum inertia/(kg•m^2)	0.4
Actuator motor speed/(r•min^{-1})	3 000
Actuator motor thrust/N	50
Band displacement/mm	40
Engagement angle/(°)	8
Tooth side pressure angle/(°)	8
Torsional stiffness/(N•m•rad^{-1})	360
Frictional torque/(N•m)	37.5

2.1 Dynamic characteristics

As shown in Fig.4, the duration of meshing stage decreases rapidly as the rotating speed increases。 It takes 0.022 s and 0.012 s at initial speeds of 75 and 120 r/min, respectively. When the initial speed is only 30 r/min, the rotating speed of the brake drum has already dropped to 0 before reaching its final position. Since the brake drum is not completely jammed, it will rotate again under the action of the motor until it collides with the limit bolt. Such a phenomenon can increase the rotating speed of the brake drum to as high as 180 r/min, resulting in a large impact torque. Thus, on the basis of Eq.(18), the initial speed of brake drum has to be greater than 50 r/min to ensure the brake reliability. As the elastic damping element can only absorb lim-

ited brake energy, the brake drum speed should not be too large. Therefore, the initial speed is set as 60, 80 and 100 r/min to investigate the dynamic characteristics of the braking process.

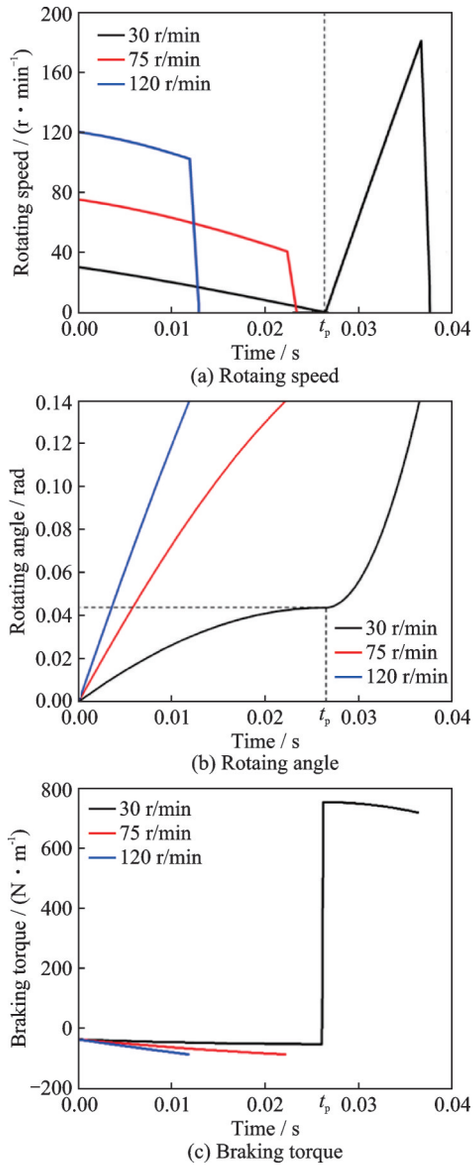

Fig.4 Dynamic characteristics at meshing stage

Fig.5 presents the braking dynamic characteristics via the mathematical calculation (MC) and the finite element method (FEM). The variation of the brake drum angle obtained by the two methods is basically consistent, and the speed error is within 2%, indicating that MC is effective to simulate the braking process. However, even though the impact toruqe of the two methods is basically the same in the first two braking stages, significant differences appears in the subsequent stages. The maximum impact torque obtained by FEM is almost twice that calculated by MC. Such a phenomenon can be related to the selection of the damping factor: The larger the damping, the smaller the impact torque. It is known that the steel damping is 0.01%—0.1% of its stiffness. Since the steel stifneess is around 200 000 N/mm, the corresponding damping range is 20—200 N·s/mm. For example, the damping coefficients are selected as 20 N·s/mm and 60 N·s/mm at 80 r/min, and the impact torque are 1 141 N·m and 833 N·m, respectively. Therefore, it is necessary to further analyze the stress properties of the brake components to verify its working reliability, where the damping coefficient is 0.01% of the stiffness.

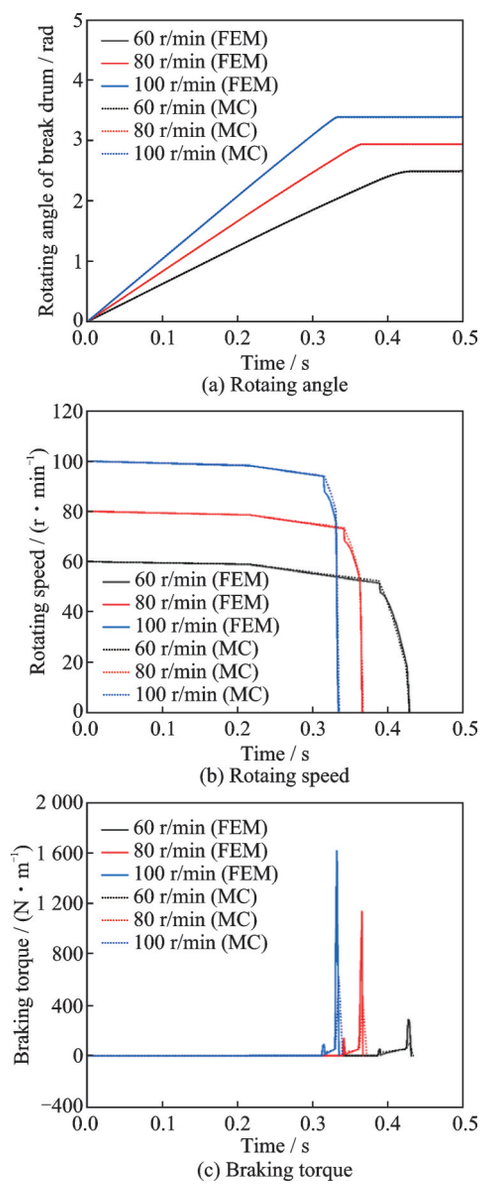

Fig.5 Braking dynamic characteristics at different initial speeds

Since the duration of gap eliminating stage keeps the same, the greater the initial speed, the larger the rotating angle of brake drum. As the drum angle is the same in the sliding stage and the meshing stage, the larger the speed, the shorter the braking time. Fig.5(b) illustrates the four stages of the braking process, where the speed decrease rate increases progressively. The duration of the gap eliminating stage is the longest, and it has little influence on the initial speed. Although the meshing stage lasts for a short time, the rotating speed decreases obviously under the action of friction force, which can effectively reduce the excessive impact torque in the collision stage.

As shown in Fig.5(c), the greater the rotating speed, the larger the impact torque in the collision stage. More exactly, the rotating speeds fall down to 18.4, 54.8, and 80.3 r/min, and the corresponding maximum impact torques are 103.9, 409.2, and 622.5 N·m, respectively. In contrast, the brake torques in the gap eliminating stage and the sliding stage are quite smaller than those who have a limited influence on the rotating speed. In order to obtain reliable and stable braking performance, the impact torque should be reduced as much as possible, thus it is advisable to reduce the rotating speed to 0 at the beginning of collision.

2.2 Stress characteristics

Fig.6 presents the stress distribution of the key components at 60 r/min. The stress is the greatest at the lower end of the two bands, where is the weak link of the brake band. As shown in Fig.6(b), the maximum bending stress position of the fork shaft is on both sides near the middle position, which is basically consistent with the installation position of the brake band on both sides. As demonstrated in Figs.6(c, d), since the two slider pins bear the shear stress from the brake band, the highest stress appears in the middle position.

As demonstrated in Fig.7, with the increase of the braking speed, the maximum stress of brake components shows an increase trend. The maximum stress increases fastest on the right brake band, followed by the left brake band and the fork shaft. The left and the right brake bands mainly bear the unidirectional compressive stress and tensile stress, while the fork shaft and the pin mainly bear bending stress. The maximum stress of the right

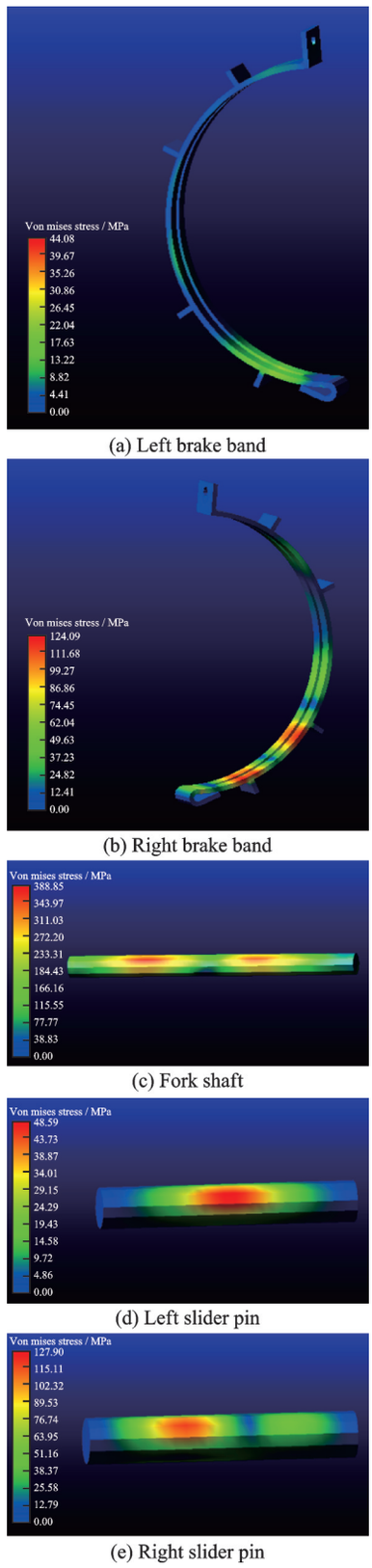

(a) Left brake band

(b) Right brake band

(c) Fork shaft

(d) Left slider pin

(e) Right slider pin

Fig.6 Stress distribution of the key components

brake band is nearly three times that of the left brake band. It may be caused by the fact that the right brake band is mainly subjected to the tensile stress. Besides, as the maximum stress of the right brake band reaches 514 MPa at 100 r/min, the tensile strength of the material should exceed 520 MPa and the maximum stress region needs to be optimized. In conclusion, the stress of each component meets engineering requirements within a reasonable range.

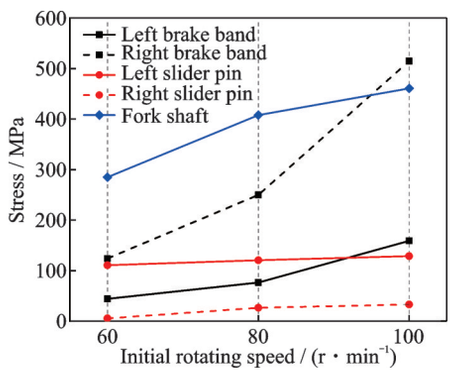

Fig.7 Maximum stress of brake components

3 Conclusions

A new electrically controlled toothed band brake is presented to satisfy the development of all-electric transmission. The mathematical model and the finite element model of the brake are proposed to study its dynamic characteristics and stress distribution at different speeds. The main conclusions obtained are as follows.

(1) The braking process can be divided into gap eliminating stage, the sliding stage, the meshing stage and the collision stage. The speed drops faster in the meshing stage and sharply turns to 0 in the collision stage. In order to reduce the impact torque and shorten the braking time, the initial speed of brake drum should be controlled within 50—100 r/min.

(2) The stress of brake components shows an increase trend with the rise of initial speed, and the maximum stress appears in the collision process. The maximum stress of the right brake band increases fastest, followed by the left brake band and the fork shaft.

References

[1] WU J P, MA B, LI H Y, et al. Creeping control strategy for direct shift gearbox based on the investigation of temperature variation of the wet multi-plate clutch[J]. Journal of Automobile Engineering, 2019, 233(14): 3857-3870.

[2] WU B Z, QIN D T, HU J J, et al. Analysis of influencing factors and changing laws on friction behavior of wet clutch[J]. Tribology International, 2021, 162: 107125.

[3] YANG L K, MA B, AHMADIAN M, et al. Pressure distribution of a multidisc clutch suffering frictionally induced thermal load[J]. Tribology Transactions, 2016, 59(6): 983-992.

[4] YU L, MA B, CHEN M, et al. Investigation on the thermodynamic characteristics of the deformed separate plate in a multi-disc clutch[J]. Engineering Failure Analysis, 2020, 110: 104385.

[5] ZHU M Y, LIU X T, KAN F C, et al. Life cycle prediction and evaluation of clutch friction plate considering wear models and thermal stress[J]. Journal of Tribology, 2021, 143(4): 041701.

[6] YANG S C, ZHOU G, HU D M, et al. Development of hydraulic continuous shifting devices for the host machine of the tunnel boring machine[J]. Engineering and Applied Sciences, 2020, 5(6): 106.

[7] HU M H, CHEN L, WANG D Y, et al. Modeling and characteristic study of the shifting engagement process in stepped transmission[J]. Mechanism and Machine Theory, 2020, 151: 103912.

[8] SHIN J W, KIM J O, CHOI J Y, et al. Design of 2-speed transmission for electric commercial vehicle[J]. International Journal of Automotive Technology, 2014, 15(1): 145-150.

[9] RAHIMI MOUSAVI M S, PAKNIYAT A, WANG T, et al. Seamless dual brake transmission for electric vehicles: Design, control and experiment[J]. Mechanism and Machine Theory, 2015, 94: 96-118.

[10] BÓKA G, MÁRIALIGETI J, LOVAS L, et al. Face dog clutch engagement at low mismatch speed[J]. Periodica Polytechnica Transportation Engineering, 2010, 38(1): 29.

[11] DUAN C W. Analytical study of a dog clutch in automatic transmission application[J]. SAE International Journal of Passenger Cars-Mechanical Systems, 2014, 7(3): 1155-1162.

[12] ANDERSSON M, GOETZ K. FE analysis of a dog clutch for trucks withall-wheel-drive[D]. Växjö, Sweden: Linnaeus University, 2013.

[13] HAN D S, HAN G J, CHOI D H. A study on durability enhancement of band brake for mooring winch[J]. Advanced Materials Research, 2011, 201/202/203: 314-317.

[14] DOWNEY A, CAO L, LAFLAMME S, et al. High capacity variable friction damper based on band brake technology[J]. Engineering Structures, 2016, 113: 287-298.

[15] LI Yaxi, MA Biao, LI Heyan, et al. Research of the shifting characteristic of planetary transmission with using tooth brake[J]. Mechanical Transmission, 2017, 41(12): 49-53. (in Chinese)

[16] MA Biao, WANG He, ZHENG Changsong, et al. Study on braking characteristics of the new tooth band brake[J]. Transactions of Beijing Institute of Technology, 2022, 42(4): 398-406. (in Chinese)

[17] MA Biao, WANG He, ZHANG Cunzhen, et al. Analysis on working characteristics of non-full-tooth meshing for tooth band brake[J]. Journal of Machine Design, 2021, 38(10): 28-35. (in Chinese)

Acknowledgements This work was funded by the National Natural Science Foundation of China (Nos.52205047, 52175037), China Postdoctoral Science Foundation (No. 2021M700422), and Beijing Key Laboratory Foundation (No.KF20212223201).

Authors

The first author Mr. **LI Chao** obtained his bachelor's degree in armored vehicle engineering and master's degree in mechanical engineering from Beijing Institute of Technology. He is now a Ph.D. candidate in mechanical engineering. His research directions include vehicle transmission reliability theory, hydraulic lubrication system pollution control, fault diagnosis, dynamic modeling and analysis, wear and deformation mechanism, and fault diagnosis for the wet multi-disc shifting clutch, intelligent operation and maintenance technology.

The corresponding author Dr. **CHEN Man** recieved his PH.D. degree from Beijing Institute of Technology. He is an associate professor and master's supervisor at School of Mechanical and Vehicle Engineering, Beijing Institute of Technology. His professional field is vehicle engineering, and his main research directions include the theory and methods of automatic control of vehicle transmission, as well as methods and technologies for comprehensive information processing of vehicles.

Author contributions Mr. **LI Chao**, Mr. **LI Kai** and Dr. **CHEN Man** designed the study, complied the models, conducted the analysis, interpreted the results and wrote the manuscript. Mr. **FAN Ye** and Ms. **ZHOU Ruyi** contributed to the discussion. Mr. **LU Weichen** contributed to the background of the study. All authors commented on the manuscript draft and approved the submission.

Competing interests The authors declare no competing interests.

(Production Editor: ZHANG Bei)

一种新型电动齿形带式制动器动力学特性研究

李 超[1], 李 凯[1], 陈 漫[1], 范 晔[1], 周如意[2], 卢玮辰[3]

(1.北京理工大学机械工程学院,北京 100081, 中国;
2.中国北方汽车研究所,北京 100072, 中国;
3.上海船用柴油机研究所,上海 201108, 中国)

摘要:本文提出了一种基于两挡行星变速机构的新型电动齿形带式制动器,建立了制动过程的动力学数学模型和有限元模型,研究了制动带与制动齿之间的动力学特性,以及制动部件的应力分布特征。根据带式制动器的结构特点和工作原理,制动过程可分为消除间隙阶段、滑动阶段、啮合阶段和碰撞阶段。制动鼓初始转速越大,碰撞阶段冲击扭矩越大,制动部件应力越大,初始转速的理想范围为50~100 r/min,极限应力出现在右制动带上,达到了514 MPa。本文为两挡变速机构全电化研究和电动齿形带式制动器的应用提供了理论基础。

关键词:齿形带式制动器;电气控制;制动特性;转速;冲击扭矩值